American Mineralogist, Volume 79, pages 513–525, 1994

Contact metamorphism surrounding the Alta stock: Thermal constraints and evidence of advective heat transport from calcite + dolomite geothermometry

STEPHEN J. COOK,* JOHN R. BOWMAN
Department of Geology and Geophysics, University of Utah, Salt Lake City, Utah 84112, U.S.A.

ABSTRACT

Metamorphism of the siliceous dolomites in the contact aureole of the mid-Tertiary Alta stock has produced a series of isograds with increasing metamorphic grade: talc, tremolite, forsterite, clinohumite, and periclase. Calcite + dolomite geothermometry applied to 30 samples of these dolomites indicates that the prograde metamorphism occurred over the approximate temperature range 410–575 °C for the tremolite-bearing through periclase-bearing zones. The calcite + dolomite temperatures follow a consistent trend of increasing temperature in the direction of the intrusive contact. Consistency between this temperature regime and the positions of the T-X_{CO_2} phase equilibria applicable to the prograde reactions requires a minimum fluid pressure of 75 MPa during the metamorphic event. Comparisons between the peak temperature-distance profile defined by the calcite + dolomite data and temperature-distance profiles calculated from geologically reasonable, two-dimensional conductive cooling models of the stock suggest that the temperature regime in the southern portion of the Alta aureole was affected significantly by advective heat transfer. Field, petrologic, and whole-rock stable isotopic data, as well as the results of stable isotope transport modeling, are consistent with this possibility and require further that the fluid flow responsible for this advection was lateral to the intrusive contact.

INTRODUCTION

There are now several heuristic thermal modeling studies that have shown that fluid infiltration can affect significantly the thermal regime surrounding a cooling pluton and consequently the spatial and temporal evolution of its isotherms (e.g., Cathles, 1977; Norton and Knight, 1977). This same fluid infiltration can also play an important, and often interrelated, role in controlling the progress of mixed-volatile reactions and hence the prograde T-X_{CO_2} path of progressive metamorphism of siliceous carbonate-bearing rocks in these aureoles (e.g., Moore and Kerrick, 1976; Bowman and Essene, 1982; Ferry, 1983, 1989; Nabelek et al., 1984; Bebout and Carlson, 1986). During progressive metamorphism of siliceous carbonate-bearing rocks, fluid infiltration competes with the buffering capacity of the metamorphic reactions for control of pore fluid composition (Rice and Ferry, 1982). Yet reaction progress and pore fluid composition are also influenced by the rate and extent of the temperature increase experienced by a metamorphic rock. For contact metamorphism, this increase is controlled by the thermal budget of the aureole, which is a function of the supply of heat available (from the size of the intrusion, heat of crystallization, and temperature of the magma), of the geometry of the intrusion, of the thermal properties of the magma and rocks (crystallized pluton and surrounding country rocks), and of the primary mechanism of heat transfer (e.g., conduction vs. advection) operating in the stratigraphic section containing the reactive mineral assemblages.

Hence any quantitative evaluation of the role either of fluid infiltration in influencing the progress of metamorphic reactions or of advection in the heating of contact aureoles requires independent definition of temperature in the contact aureole. One method for establishing the required temperature control in aureoles that contain siliceous dolomites is calcite + dolomite solvus geothermometry. Although applications of this geothermometer have been frustrated by significant retrograde reequilibration of calcite in regional metamorphic terranes (e.g., Valley and Essene, 1980; Anovitz and Essene, 1987; Essene, 1989), this geothermometer has been successfully applied in contact metamorphic environments (e.g., Rice, 1977; Bowman and Essene, 1982; Hover-Granath et al., 1983).

The siliceous dolomites in the contact aureole of the Alta stock exhibit a well-developed progressive metamorphic sequence that is well suited for study using calcite + dolomite geothermometry. This study focuses on the application of calcite + dolomite geothermometry to document the thermal regime of the metamorphism that produced this sequence and to determine whether there is evidence of significant advective heat transport that accompanied the prograde metamorphism.

* Present address: Environ Corporation, 1980 Post Oak Boulevard, Suite 2120, Houston, Texas 77056, U.S.A.

0003–004X/94/0506–0513$02.00

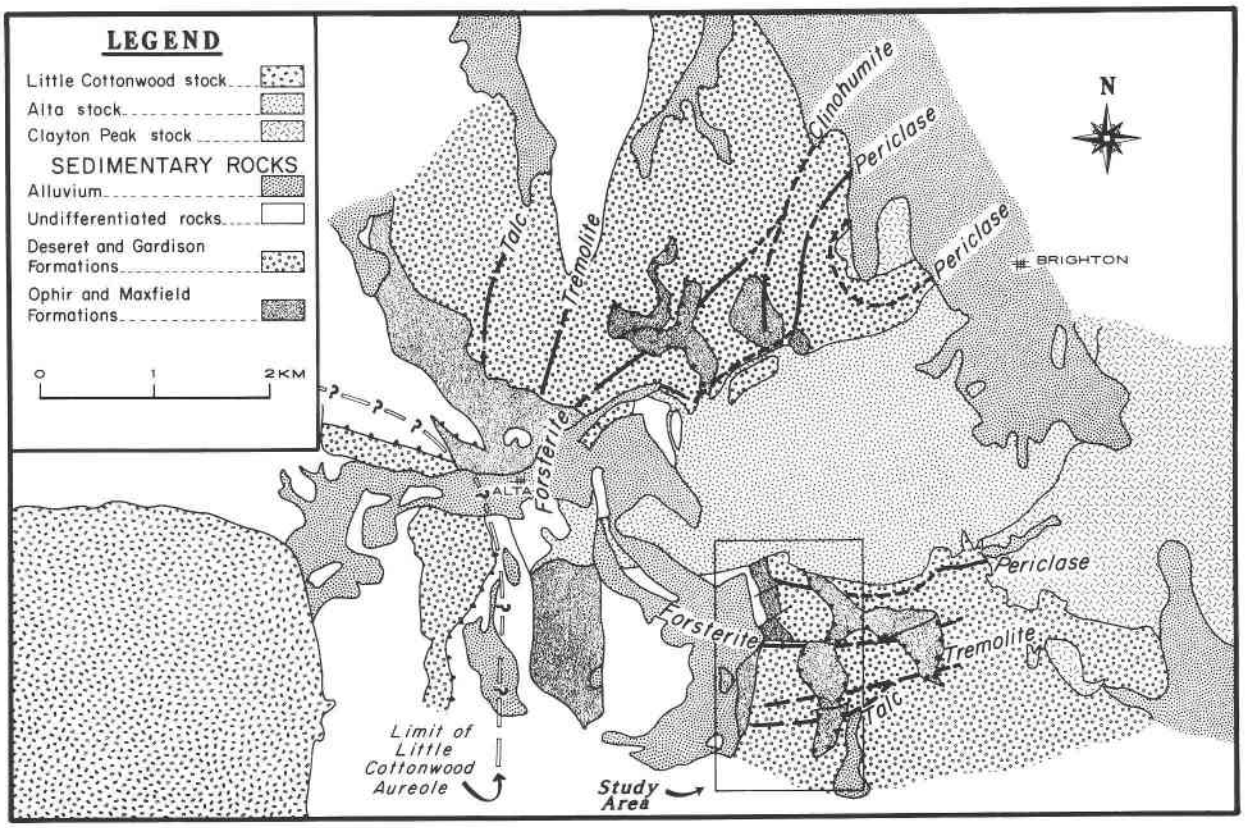

Fig. 1. Geologic map of the Alta contact aureole (Baker et al., 1966; Crittenden, 1965). Isograd locations based on mineral assemblages in the massive dolomites (Moore and Kerrick, 1976). The preintrusive Alta-Grizzly thrust fault system repeats part of the Paleozoic carbonate section both north and south of the Alta stock. This study focuses on the metamorphism along the south-central margin of the Alta stock (box labeled study area).

Geology

The Alta stock (granodiorite: Wilson, 1961) is one of several mid-Tertiary plutons (38 Ma: Crittenden et al., 1973) in Utah's central Wasatch range (Fig. 1). The stock has intruded and contact metamorphosed a sequence of Precambrian and Paleozoic sedimentary rocks consisting primarily of quartzites (Precambrian Big Cottonwood and Cambrian Tintic Formations) and a single pelitic unit (Cambrian Ophir Formation) capped by carbonate rocks (Cambrian Maxfield and Mississippian Fitchville, Deseret, and Gardison Formations). Within the study area, preintrusive thrusting (Alta-Grizzly thrust zone, Figs. 1 and 2) has resulted in the repetition of a portion of the carbonate section, placing Cambrian Maxfield over the upper Mississippian Deseret-Gardison Formations.

The south contact of the Alta stock is exposed over a vertical interval of approximately 550 m; its outcrop pattern over this interval indicates that, with small-scale, local exceptions, it is subvertical (Fig. 1). An additional 500 m of vertical relief on this contact can be inferred from exposures in mine workings in the area (Calkins and Butler, 1943). The bulk of the subsurface contact is with the Precambrian section, but the exposed contact is predominantly with the Cambrian and Mississippian carbonate rocks (Fig. 1). The metamorphism associated with the stock has affected the country rocks on the south (Maxfield, Deseret, and Gardison Formations, Figs. 1 and 2) up to approximately 2 km from the intrusive contact.

Two additional mid-Tertiary plutons are exposed in the vicinity of the Alta aureole. To the east, the Alta stock has intruded the older (42 Ma) Clayton Peak stock (granodiorite). Several kilometers to the west is the younger (32 Ma) Little Cottonwood stock (quartz monzonite). Moore and Kerrick (1976) reported overprinting of the western margin of the Alta aureole by the contact aureole of the Little Cottonwood stock.

Contact metamorphism

This study focuses on the metamorphism along the south-central margin of the Alta stock (Fig. 1). This portion of the contact aureole was selected for study because of its well-developed prograde metamorphic sequence within the dolomitic marbles (Moore and Kerrick, 1976), its simple structure and excellent exposures of the carbonate units, which allow reliable tracing of individual rock units up metamorphic grade, and a position unaf-

TABLE 1. Prograde reactions in dolomitic marbles

$$3\ Do + 4\ Qz + H_2O = Tc + 3\ Cc + 3CO_2 \quad (1)$$
$$2\ Tc + 3\ Cc = Tr + Do + H_2O + CO_2 \quad (2)$$
$$5\ Do + 8\ Qz + H_2O = Tr + 3\ Cc + 7CO_2 \quad (3)$$
$$Tr + 11\ Do = 8\ Fo + 13\ Cc + 9CO_2 + H_2O \quad (4)$$
$$4\ Fo + Do + H_2O = Chm + Cc + CO_2 \quad (5)$$
$$Do = Per + Cc + CO_2 \quad (6)$$

fected by metamorphism associated with the Clayton Peak stock to the east (Smith, 1972) and the Little Cottonwood stock to the west (Moore and Kerrick, 1976).

In the study area (Figs. 1 and 2), prograde metamorphism of the SiO_2-undersaturated siliceous dolomites has resulted in the successive appearance of talc (Tc), tremolite (Tr), forsterite (Fo), clinohumite (Chm), and periclase (Per) (Moore and Kerrick, 1976). The periclase has now been replaced by retrograde brucite (Br). These index minerals, with in most cases extensive amounts of calcite, are produced by a series of prograde metamorphic reactions that are summarized in Table 1, Reactions 1–6, and which have been discussed previously by Moore and Kerrick (1976). The unmetamorphosed equivalents of the marbles in the aureole consist predominantly of dolomite (Do) with minor quartz (Qz) and calcite (Cc) (both typically <10 modal%). Hence prograde metamorphism has produced abundant coexisting calcite and dolomite pairs throughout most of the thermal aureole. Exceptions are the innermost periclase zone, where dolomite is virtually exhausted, and in the talc zone, where only small amounts of generally fine-grained calcite exist at the margins of chert nodules.

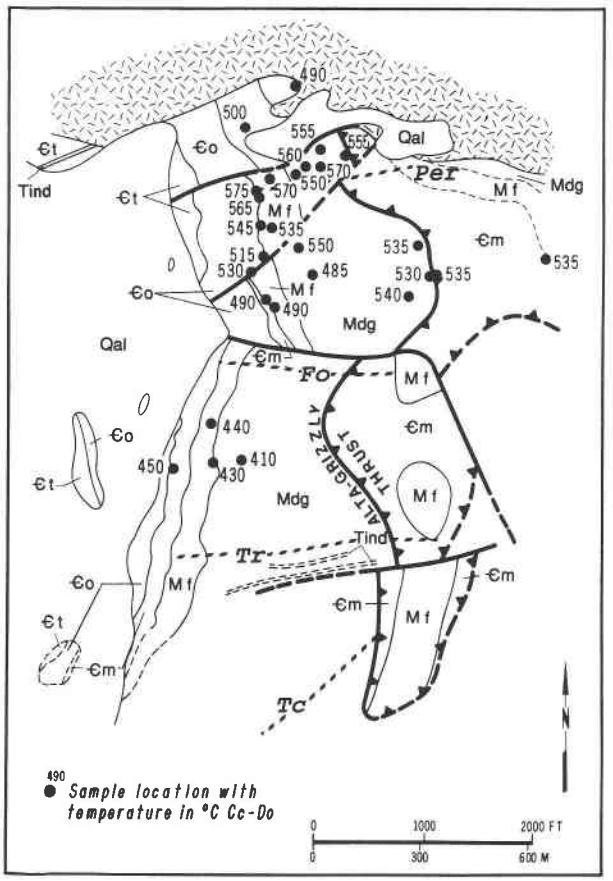

Fig. 2. Geologic map of the study area with sample locations and calcite + dolomite geothermometry results. Peak temperatures (°C) recorded by coexisting calcite + dolomite pairs (data from Table 2), calculated from the equation of Anovitz and Essene (1987). Metamorphic isograds labeled by index mineral: talc (Tc); tremolite (Tr); forsterite (Fo); and periclase (Per). Geologic units are Ct = Tintic; Co = Ophir; Cm = Maxfield; Mf = Fitchville; Mdg = Deseret and Gardison; Tind = intermediate dikes; Qal = alluvium. Alta stock shown by random bar pattern. The preintrusive Alta-Grizzly thrust (labeled) has repeated part of the carbonate section.

ANALYTICAL PROCEDURES

Sample selection

Ubiquitous textural relationships document the coexistence of equilibrium calcite + dolomite pairs at all metamorphic grades. Samples for geothermometry were selected from unweathered field specimens that lacked obvious evidence of alteration of primary metamorphic minerals. Thin sections of these samples were then stained with alizarin red to verify the existence of coexisting calcite and dolomite. Samples containing suitable calcite + dolomite pairs were then examined optically (400× magnification) for evidence of dolomite exsolution from calcite.

Exsolved dolomite was not observed in any of the tremolite zone calcite grains nor in most of the samples from the forsterite zone; however, several samples from the highest grade forsterite zone and virtually all periclase zone samples contain individual calcite grains that exhibit minor exsolved dolomite. For geothermometry measurements, the least affected samples from the inner forsterite and periclase zones were chosen for analysis.

Analytical methods

Calcite analyses were performed on the Cameca SX-50 electron microprobe at the University of Utah. A 15-keV beam current, which is required to detect Fe, and a 20-nA sample current, which was chosen to avoid volatilization of Mg, were used to obtain the analyses. Multiple analyses of single points were performed on many samples by reducing the beam diameter from 30 to 10 μm in 10-μm steps to confirm the absence of Mg volatilization. For most analyses, a 30-μm beam diameter was used to reintegrate potential submicroscopic-scale exsolution. Various smaller beam sizes were used on the tremolite zone samples because the calcite grains were too small to use a 30-μm beam. Element concentrations were calculated from relative peak intensities using the $\phi(\rho Z)$ algorithm of Pouchou and Pichoir (1991).

Analytical results

The compositions of calcite grains coexisting with dolomite were determined on 30 samples (Table 2). Rep-

TABLE 2. Geothermometry data

Zone	Sample	N	Mean $MgCO_3$	Sd	Std. err.	Max. $MgCO_3$	T (°C) mean	T (°C) max.
Per	88.3	24	5.48	0.59	0.12	6.20	545	570
	88.14	26	4.99	0.49	0.10	5.72	525	555
	88.40	28	3.28	0.30	0.06	4.14	445	490
	88.51	30	4.29	0.69	0.13	5.59	495	550
	88.A5*	20	3.49	0.27	0.06	3.97	460	480
	88.A7*	30	3.47	0.45	0.08	4.38	455	500
	88.B6	26	5.08	0.57	0.11	6.12	530	570
	90.2	25	4.60	0.60	0.12	5.68	510	555
	90.4b	26	5.54	0.36	0.08	5.93	550	560
Fo	88.7	26	5.62	0.22	0.04	5.98	550	565
	88.8	22	5.10	0.72	0.15	6.40	530	575
	88.16	28	4.80	0.43	0.08	5.48	520	545
	88.18	24	4.23	0.66	0.13	5.06	495	530
	88.20	23	3.16	0.41	0.09	4.17	440	490
	88.33	33	4.08	0.42	0.07	5.16	490	535
	88.55	27	5.12	0.23	0.04	5.59	530	550
	88.60**	11	4.50	0.40	0.12	5.25	505	535
		32	2.54	0.58	0.10	3.35	395	450
	88.C2*	22	3.17	0.44	0.09	4.17	440	490
	88.C5*	34	3.16	0.55	0.09	4.14	440	490
	88.D2*	22	3.05	0.39	0.08	3.85	430	475
	88.D8*	30	2.94	0.45	0.08	4.00	425	485
	90.7	25	3.75	0.44	0.08	4.75	470	515
	90.13b	27	4.23	0.45	0.09	5.19	495	535
	90.18c	30	3.02	0.80	0.15	5.08	430	530
	90.19	25	4.15	0.52	0.10	5.14	490	535
	90.21	30	3.57	0.81	0.15	5.31	460	540
Tr	89.10	25	2.89	0.45	0.09	3.32	420	450
	89.16b	28	1.54	0.68	0.13	3.03	290	430
	89.20	26	1.39	0.77	0.15	2.69	265	410
	89.24a	24	2.16	0.74	0.15	3.23	365	440

Note: maximum, mean, standard deviation, and standard error of weight percent $MgCO_3$ in calcite. Number of individual grains analyzed per sample is given by *N*.

* Results of *t*-test comparisons for sample pairs from the same outcrop: A5 vs. A7, $t = 0.18$; C2 vs. C5, $t = 0.07$; D2 vs. D8, $t = 0.90$; $t_{0.1} > 1.282$ required to reject.

** Sample 88.60 exhibits a bimodal distribution. Values reported for two distributions.

TABLE 3. Calcite analyses

Zone Sample	Per 88.3	Per 90.4b	Fo 88.8	Fo 88.33	Tr 89.16b	Tr 89.24a
CaO	53.13	53.15	52.78	53.34	54.75	54.54
MgO	2.50	2.41	2.57	2.09	1.21	1.31
FeO	0.03	0.00	0.09	0.02	0.05	0.03
MnO	0.00	0.02	0.03	0.05	0.00	0.01
CO_2	44.44	44.35	44.30	44.17	44.32	44.26
Total	100.10	99.93	99.76	99.65	100.33	100.15
$CaCO_3$	93.81	94.04	93.50	94.76	96.95	96.71
$MgCO_3$	6.15	5.93	6.33	5.16	2.98	3.23
$FeCO_3$	0.04	0.00	0.12	0.02	0.07	0.04
$MnCO_3$	0.00	0.03	0.04	0.05	0.00	0.02

Note: oxides reported in weight percent, carbonate end-members in mole percent normalized to 100.

resentative analyses of calcite are listed in Table 3. A minimum of 20 calcite grains were analyzed in each sample. The data in Table 2 summarize the results of these single point analyses on individual calcite grains from each sample.

Multiple point analyses were performed on a number of calcite grains in each sample to test their submicroscopic homogeneity and chemical zonation. The intragranular compositional variation of the individual grains examined was <0.3 wt% Mg in all samples and was typically <0.2 wt%. No systematic chemical zoning was observed in any sample. However, because of the relatively large beam diameter chosen for our analytical procedure, any chemical zoning that might exist in the outermost portions of the calcite grains (≤ 50 μm from grain edge) could not be identified.

Almost all samples exhibit significant grain to grain variations in Mg content that exceed significantly the variation in Mg content within individual grains (at least in grain interiors). Such variations are usually attributed to retrograde equilibration (Rice, 1977; Valley and Essene, 1980; Bowman and Essene, 1982; Hover-Granath et al., 1983; Anovitz and Essene, 1987; Essene, 1989). Retrograde equilibration produces calcite grains with Mg contents lower than those defined at peak metamorphic temperatures. Averaging all data incorporates such retrograde effects and therefore underestimates significantly the actual peak temperature experienced by a sample. This is a serious problem in slower-cooled regional metamorphic terranes. At Alta, retrogradation has also clearly affected many of the samples from the periclase zone because even maximum temperatures preserved in these samples (Table 2) are lower than temperatures defined in the inner forsterite zone still farther away from the intrusion (the heat source) and are significantly lower than minimum temperatures (575 °C) required by phase equilibrium limits for periclase stability (see below). Because the signal of interest is peak temperature, we utilize the maximum Mg content (maximum T) recorded in each sample as the most valid indicator of the peak metamorphic temperature for the following discussions. Because of the potential effects of retrogradation, even the maximum temperatures preserved in a sample must be viewed as minimum estimates of actual peak metamorphic temperatures.

Reported temperatures (Table 2) were calculated using the calcite + dolomite geothermometry expression of Anovitz and Essene (1987). The applicable range of this expression is 250–800 °C. Uncertainty in these temperatures due to the calibration of the geothermometry expression and to analytical uncertainty is estimated to be ±50 °C for temperatures below 500 °C and ±25 °C above 500 °C. Temperatures in Table 2 are rounded to the nearest 5 °C.

To evaluate outcrop-scale equilibration, sample pairs from three outcrops were tested for consistency between their compositional distributions (Table 2). The mean calcite compositions of the samples were compared statistically using a Student's t distribution. In all three cases, the sample means were found to be not statistically different at a confidence level of 0.9. These results are consistent with the attainment of thermal equilibrium by calcite + dolomite pairs on an outcrop scale.

Discussion

Thermal constraints on metamorphism

The maximum temperatures calculated for each sample are shown on a map of the study area in Figure 2 and as a function of horizontal distance from the intrusive contact in Figure 3. The temperatures range from 410 to 450 °C for the outer tremolite zone, are 490 °C for the outer forsterite zone, and reach a high of 575 °C in the inner forsterite zone near the periclase isograd (Fig. 3). These temperatures are interpreted to be minimum estimates of peak metamorphic temperatures and follow a consistent trend of increasing temperature in the direction of the intrusive contact (Fig. 3).

The maximum calculated temperatures (570–575 °C) occur on both sides of the periclase isograd in both the periclase and forsterite zones. Temperatures of 570–575 °C for the periclase zone are slightly less than those recorded for the periclase zone associated with the northern Boulder batholith (590–625 °C: Rice, 1977) and the Black Butte stock (585–600 °C: Bowman and Essene, 1982), both of which formed at depths similar to the Alta stock (P_l = 100–150 MPa).

Several periclase zone samples, particularly those close to the intrusive contact, yield temperatures considerably lower than the maximum observed temperatures. Several of these temperatures are <500 °C, which is well below the temperatures required by phase equilibria for the stability of periclase (see below) and below those (600–625 °C) typically attained in periclase-bearing zones near igneous contacts (Rice, 1977; Bowman and Essene, 1982). These large discrepancies indicate that these periclase-zone calcite grains have undergone significant retrograde reequilibration.

A second-order polynomial curve provides a good fit to the temperature-distance trend defined by the calcite + dolomite geothermometry (Fig. 3). This curve allows the contact temperature (T_c) to be estimated. The resulting value, 626 °C, represents the likely peak temperature at the igneous contact; this temperature is not a great deal higher than that at the periclase isograd (570–575 °C).

Constraints on fluid pressure during metamorphism

The thermal regime indicated by the results of calcite + dolomite geothermometry also places limits on fluid pressures (P_f) during the metamorphic event. Because the results of calcite + dolomite geothermometry are nearly independent of pressure (Anovitz and Essene, 1987), the fluid pressure regime during the metamorphic event must have been such that the T-X_{CO_2} locations of the mixed-volatile phase equilibria that define the stability field of periclase are consistent with the measured calcite + dolomite geothermometry results.

Microprobe and whole-rock chemical analyses indicate that phase equilibria in the CaO-MgO-SiO_2-H_2O-CO_2 system, after adjustment for the effects of F, can be reasonably applied to the observed mineral assemblages in the Alta contact aureole (Moore and Kerrick, 1976; Cook, 1992). The most restrictive equilibrium is Reaction 6, which was responsible for the appearance of periclase. Figure 4 illustrates T-X_{CO_2} equilibria governing the formation of periclase calculated at a constant lithostatic pressure of 150 MPa and various fluid pressures between hydrostatic (approximately 50 MPa) and lithostatic (150 MPa) pressure conditions. The lithostatic pressure (P_l) estimate, 100–200 MPa, was made by Wilson (1961) using stratigraphic measurements. However, his reconstruction is complicated by possible stratigraphic thinning over an ancestral Uinta arch or possible thickening from preintrusive thrusting. Multiple preintrusive thrusts have been mapped by Baker et al. (1966) in both the north and south sides of the Alta stock (Fig. 1). Mineral assemblages from the Ophir Formation (biotite + andalusite + potassium feldspar + quartz ± cordierite) in the innermost aureole also constrain pressures to 150 ± 50 MPa (Kemp, 1985).

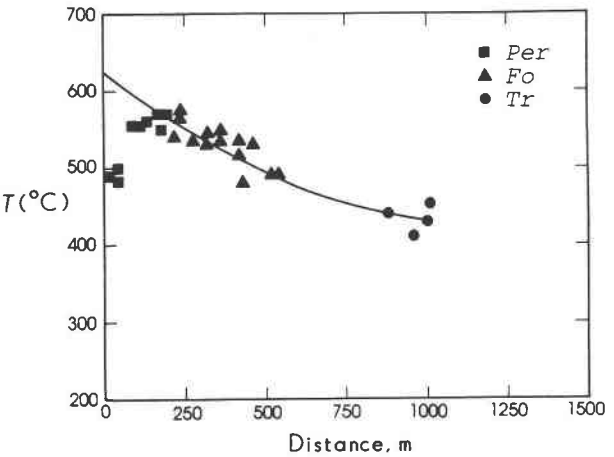

Fig. 3. Results of calcite + dolomite geothermometry plotted as a function of sample distance from the stock contact. The solid curve represents a second-order polynomial fit to the calcite + dolomite geothermometry results, excluding the lower, retrograded temperatures in the periclase zone. This fitted curve is used to represent the peak temperature-distance profile for the aureole in the text. Because the fit is good, extrapolation of the curve to the igneous contact provides a good estimate of contact temperature (T_c) = 626 °C.

The maximum temperatures recorded by calcite + dolomite geothermometry at the periclase isograd, which lies a maximum of 200 m from the intrusive contact, are 570–575 °C (Figs. 2 and 3). These temperatures require a minimum fluid pressure of approximately 75 MPa to stabilize the assemblage Per + Cc relative to Dol (Fig. 4). As most of the periclase zone samples have been affected by retrograde reequilibration, 575 °C must be considered the minimum temperature for the formation of this zone. Higher temperatures would permit correspondingly higher fluid pressures. If 575 °C is close to the actual maximum temperature achieved at the periclase isograd,

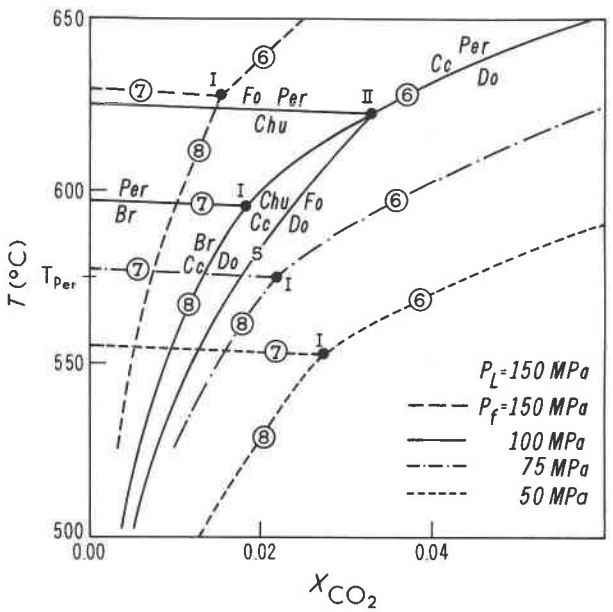

Fig. 4. T-X_{CO_2} phase equilibria governing the formation of clinohumite- and periclase-bearing mineral assemblages in the periclase zone at a constant lithostatic pressure of 150 MPa and fluid pressures of 50, 75, 100, and 150 MPa. For the estimated lithostatic pressure of 100–200 MPa for the Alta aureole (Wilson, 1961; Kemp, 1985), these fluid pressures correspond approximately to hydrostatic (50), intermediate (75–100), and lithostatic (150) pressure conditions. Reactions in addition to Reactions 5 and 6 listed in Table 1 are (7) brucite (Br) = periclase (Per) + H_2O; (8) dolomite (Do) + H_2O = calcite (Cc) + Br + CO_2. These equilibria restrict the stability of periclase to T-X_{CO_2} conditions above invariant point I and Reactions 6 and 7. Calcite-dolomite geothermometry defines a minimum temperature of 575 °C for the formation of periclase (marked T_{Per} on the temperature axis). This minimum temperature, combined with these phase equilibria, yields a minimum estimate of fluid pressure of about 75 MPa for contact metamorphism in the aureole. Equilibria were calculated using thermodynamic data from Helgeson et al. (1978), except for clinohumite, which was extracted from data of Duffy and Greenwood (1979). Unit activities were assumed for all solids except clinohumite (a_{Chm} = 0.35). Values of f_{CO_2} and f_{H_2O} were calculated using the modified Redlich-Kwong equation of Bowers and Helgeson (1983).

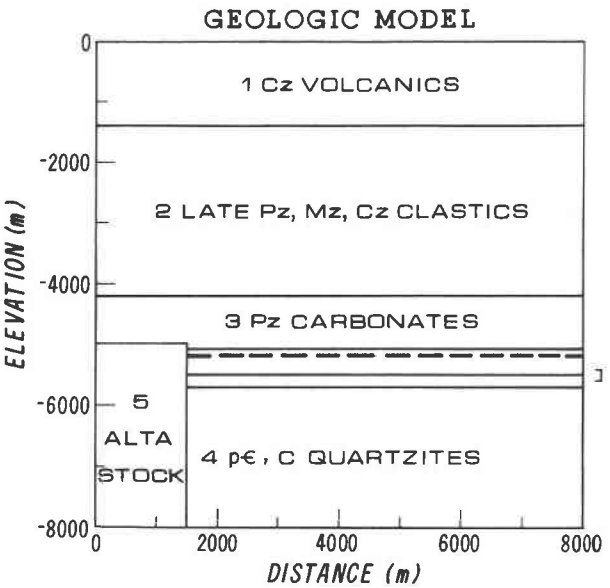

Fig. 5. Geologic model of the Alta stock and surrounding units used in the finite element simulations. Unit 1, Tertiary volcanics; Unit 2, Late Paleozoic, Mesozoic, and Cenozoic sediments; Unit 3, Paleozoic carbonate rocks; Unit 4, Precambrian and Cambrian quartzites and shales; Unit 5, Alta stock. Stock geometry, size, and location within stratigraphic section constrained by available geological field evidence. The dashed line denotes the stratigraphic position of the first Alta-Grizzly thrust fault (Fig. 2) within the study area. The bracket along the right margin indicates the stratigraphic section of carbonate rocks sampled for geothermometry (−5.4 to −5.6 km).

then metamorphism in the periclase zone must have occurred at fluid pressures below the estimated lithostatic pressure of 150 MPa.

Evidence of advective heat transfer

Moore and Kerrick (1976) have shown that the prograde metamorphic sequence exhibited by the dolomites requires infiltration by an H_2O-rich fluid with increasing metamorphic grade. In addition to driving the prograde reactions, this fluid flow may have also influenced the thermal regime surrounding the stock. Under the proper conditions, advective heat transport can significantly alter thermal regimes around cooling plutons (e.g., Cathles, 1977; Norton and Knight, 1977; Parmentier and Schedl, 1981; Furlong et al., 1991). If significant advective heat transfer occurred in conjunction with the prograde metamorphism at Alta, then evidence of this advective transport should be preserved in the peak thermal profile defined by the calcite + dolomite results (Fig. 3), which records the cooling history of the Alta stock as a function of time and distance from the margin of the stock.

To test the observed thermal profile for evidence of advective heat transfer, a conductive cooling model of the Alta stock was constructed using the finite-element method (Cook, 1992). The evolution of the thermal regime surrounding the stock is governed by the heat-transport equation:

$$\frac{\partial}{\partial x_i}\left(\lambda_{ij}\frac{\partial T}{\partial x_j}\right) = [\phi\rho_f C_f + (1-\phi)\rho_s C_s]\frac{\partial T}{\partial t} \qquad (9)$$

in which T represents the temperature, C_f and C_s the specific heat capacities of the fluid and solid, respectively, ρ_s the solid density, ϕ the porosity, and λ_{ij}^s the thermal conductivity tensor of the solid-fluid composite

$$\lambda_{ij} = \phi\lambda^f + (1-\phi)\lambda_{ij}^s.$$

The governing partial differential Equation 9 was solved numerically using the Galerkin finite-element method (Huyakorn and Pinder, 1983) applied over triangular elements.

The geologic model used in the simulations is illustrated in Figure 5. The model is divided into five distinct rock units, based on the observed stratigraphic and structural relationships surrounding the stock, reported subsurface geology (Calkins and Butler, 1943; Baker et al., 1966), and late Paleozoic, Mesozoic, and Cenozoic stratigraphy from elsewhere in the central Wasatch range (Wilson, 1961; Hintze, 1973).

Units 1 through 4 constitute the stratigraphic section into which the stock was emplaced. Unit 1 consists of volcanic rocks, roughly equivalent in age to the stock; Unit 2, a package of clastic sediments, predominantly of Mesozoic and Cenozoic age; Unit 3, the Paleozoic siliceous dolomites exposed in the contact aureole; and Unit 4, the Precambrian and Cambrian quartzites and shales that make up the bulk of subsurface contact length of the Alta stock. The section of the model that corresponds to the stratigraphic section that was sampled in the contact aureole for calcite + dolomite geothermometry is indicated by the bracket along the right margin in Figure 5. The dashed line within Unit 3 denotes the location of the Alta-Grizzly thrust zone (Fig. 2).

Unit 5 represents the Alta stock. The mapped exposure of the Alta stock (Fig. 1) has an approximate aspect ratio of 2:1 and a half-width of approximately 1.5 km. As this geometry more closely approximates a cylinder than an infinite slab, the axisymmetric form of Equation 1 was used in the models, rather than the planar coordinates that have been typically used in heuristic model studies of cooling plutons (Cathles, 1977; Norton and Knight, 1977). Outcrop patterns indicate that the southern portion of the igneous contact is nearly vertical and has no major irregularities. There is no geologic evidence for an outward-dipping igneous contact nor for the presence of significant amounts of igneous material in the form of sills or dikes extending any great distance into the aureole beneath or within the marble section. The emplacement depth (5 km) is based on the stratigraphic reconstruction by Wilson (1961) and is consistent with more recent petrologic and fluid inclusion studies of the skarns and metapelites in the aureole (Kemp, 1985) and of the Alta stock (John, 1991).

In the model, mean values were used for thermal conductivities (λ_s) and specific heat capacities (C_s) for each stratigraphic unit (Table 4). Thermal conductivities are based on compiled values for rocks of analogous composition (Carslaw and Jaeger, 1959; Woodside and Messmer, 1961); heat capacities are based on heat capacities for minerals (Robie et al., 1978) and mineral modes for the rock units. The values of λ_s and C_s were also chosen for the individual units on the basis of their average temperature under a conductive steady-state geothermal gradient with a basal heat flux of 100 mW/m² and a mean surface temperature of 10 °C. This approach is consistent with the results of numerical experiments conducted by Giberti et al. (1984), which indicate that mean values can be used as reasonable approximations for the properties of the solids (i.e., heat capacities, thermal diffusivities) because they are relatively insensitive to changes in pressure and temperature. For the stock (Unit 5), an additional 300 J/(kg·°C) has been added to the heat capacity of the rocks to account for the latent heat of crystallization of the magma.

TABLE 4. Thermal parameters

Unit	ϕ	ρ_s	λ_{ij}^s	C_s
1	10.0	2700	2.0	950
2	10.0	2700	2.2	1000
3	5.0	2700	2.0	1050
4	0.5	2700	3.0	1100
5	0.5	2700	1.8	1450*

Note: ϕ = porosity (in percent), ρ_s = density (kg/m³), λ_{ij}^s = thermal conductivity [W/(m·°C)], C_s = specific heat capacity [J/(kg·°C)].

* C_s for Unit 5 (intrusion) = 1150 J/(kg·°C) + 300 J/(kg·°C) to account for latent heat of crystallization.

In contrast to the solid properties, parameter sensitivity studies conducted by Straus and Schubert (1977) demonstrate that explicit account must be taken of the pressure-temperature dependence of the properties of H_2O, as variations in these parameters affect significantly the thermal regimes in both conductively and advectively cooled systems.

Accordingly, the model accounts for the changes in the thermal properties of the pore fluids. The calculations assume that the pore fluid is pure H_2O. This neglects possible effects of a potentially significant CO_2 component in the fluid and of salinity on fluid properties. This assumption is however unavoidable, as a comprehensive set of equations describing the transport properties of both high-salinity and mixed-volatile fluids has not yet been developed.

Fluid densities for liquid H_2O were calculated using the equations of Meyer et al. (1967) for temperatures below the critical temperature and those of Keenan et al. (1978) elsewhere. Specific heat capacities were computed using the expressions of Keenan et al. (1978) and thermal conductivities from the formulation of Kestin (1978).

Initial and boundary conditions are required to obtain specific solutions to the governing differential equation. These boundary conditions are

$$\lambda_{xx}\frac{\partial T}{\partial x} = 0 \text{ mW/m}^2 \qquad \text{for } -8 \text{ km} \le z \le 0 \text{ km at } x = 0 \text{ km and } x = 8 \text{ km}$$

$$\lambda_{zz}\frac{\partial T}{\partial z} = 100 \text{ mW/m}^2 \qquad \text{for } 0 \text{ km} \le x \le 8 \text{ km at } z = -8 \text{ km}$$

$$T = 10 \text{ °C} \qquad \text{for } 0 \text{ km} \le x \le 8 \text{ km at } z = 0 \text{ km}$$

corresponding to insulating conditions along the vertical subsurface boundaries; a constant conductive heat flux of 100 mW/m² applied along the subsurface boundary, representing an elevated regional preintrusive heat flow,

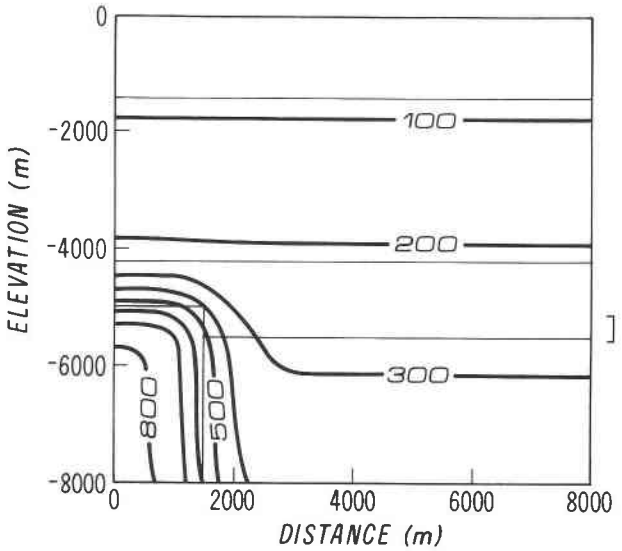

Fig. 6. Conductive cooling model at 5000 yr following emplacement of the Alta stock. The emplacement temperature of the stock was 825 °C. The bracket along the right margin denotes the stratigraphic section corresponding to the exposed contact aureole (−5.1 to −5.6 km). The carbonate section sampled for geothermometry corresponds to the deeper portion of this section, the interval −5.4 to −5.6 km.

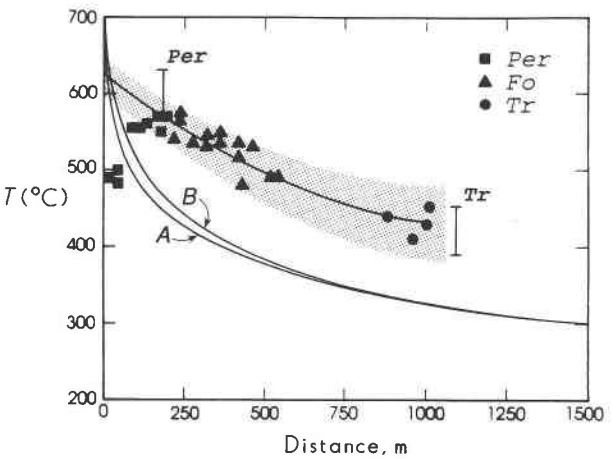

Fig. 7. Comparison between geothermometry results (Fig. 3) and peak temperature profiles (curves A and B), corresponding to the model illustrated in Fig. 6. Curves A and B define maximum model temperatures achieved along a horizontal profile at −5.5 km during 100 000 yr of cooling for initial intrusion temperatures of 825 (curve A) and 925 °C (curve B). Maximum temperature at the igneous contact corresponds to those (825 and 925 °C) obtained instantaneously upon intrusion. The −5.5-km level corresponds to the average depth of the stratigraphic interval sampled for geothermometry in the contact aureole. Also shown is the second-order polynomial fit to the geothermometry data (solid line) and a stippled band centered on this fitted curve based on estimated uncertainties in the geothermometry results of ±25 °C above 500 °C and ±50 °C below 500 °C. Brackets denote temperature limits at the positions of the periclase (Per) and tremolite (Tr) isograds based on geothermometry results and phase equilibria (Cook, 1992; this study).

which is consistent with a region experiencing periodic intrusive events; and a constant temperature of 10 °C at the surface boundary, representing a mean annual temperature. The assumption of constant heat flux across the entire base of the model leads to some overestimate of wall-rock temperatures near the igneous contact after intrusion.

The model treats the stock as if it were injected instantly at 825 °C into hydrostatically pressured, H_2O-saturated country rocks under a steady-state conductive geothermal gradient. Although instantaneous injection is geologically unrealistic, this approach is considered acceptable, as upward migration rates of thermal maxima are significantly less than the rates of igneous intrusion (Norton and Knight, 1977).

The emplacement temperature estimated for the stock (825 °C) is based on the results of zirconium geothermometry (Watson and Harrison, 1983) applied to whole-rock analyses of the Alta stock (maximum whole-rock zirconium content 220 ppm) and is consistent with its granodiorite bulk composition (Cook, 1992). This geothermometer assumes that 100% of the whole-rock zirconium was initially present in the liquid portion of the magma. Thus this approach yields a maximum temperature estimate for the stock because of the possibility of inherited zircon from the source region. In addition, John (1991) has applied empirical biotite crystallization geothermometry to biotite compositions from the Alta stock. For all samples from buffered assemblages, biotite crystallization temperatures ranged from 650 to 840 °C, with most results in the range 700–800 °C. These results are consistent with the emplacement temperature estimate based on zirconium geothermometry.

The effect of the endothermic metamorphic reactions that occurred in the marbles and underlying pelitic rocks (Figs. 1 and 2) on the thermal evolution of the aureole has not been incorporated into the model. Ferry (1980) has noted that metamorphic reactions can, depending on bulk composition and mineral assemblage, consume a significant quantity of heat. The effect of these endothermic reactions is to lower temperature throughout the aureole. Numerical experiments by Bowers et al. (1990) suggested that temperatures may be overestimated by as much as 40–50 °C if the effect of endothermic reactions is ignored. Thus the calculated temperature regimes presented in this study should be regarded as maximum estimates.

Figure 6 illustrates the results of the cooling model at 5000 yr following emplacement of the stock. A peak temperature-distance profile, corresponding to this model over a span of 100 000 yr, is shown as curve A in Figure 7. This model profile was taken at a depth of −5.5 km, which corresponds to the average depth of the stratigraphic section sampled for geothermometry in the contact aureole (i.e., data of Fig. 3).

A comparison in Figure 7 between the model profile (curve A) and the observed peak temperature-distance profile based on a second-order polynomial fit to the calcite + dolomite data from Figure 3 indicates that this conductive model fails to achieve the observed peak temperatures at virtually all distances; observed temperatures are significantly greater than model temperatures (typically >100 °C beyond the first 100 m from the igneous contact) at all distances. This is a result of the rapid cooling of the upper portion of the stock that occurs within the first few hundred years following its emplacement. In the model, the minimum temperature required by geothermometry and phase equilibria for the formation of periclase (575 °C) was achieved only within 15 m of the intrusive contact, a distance much less than the observed maximum distance of 200 m (bracket labeled Per). The discrepancies between model results and the geothermometry data exceed the uncertainties in the geothermometry data (stippled band centered on the regression curve in Fig. 7).

One possible explanation for these discrepancies is that the actual emplacement temperature of the stock was greater than the temperature estimated by zirconium geothermometry (825 °C). Curve B in Figure 7 represents an analogous peak temperature profile for a conductive model in which the emplacement temperature was set at 925 °C. The increased intrusion temperature has relatively little effect on the model thermal profile, and there remain large discrepancies between observed and model temperatures throughout the aureole. The predicted width of the periclase zone does increase slightly to approximately 25 m. This modest improvement implies that to achieve the observed width of the periclase zone ($T \geq 575$ °C up to 200 m from the intrusive contact) using strictly conductive heat transfer would require a model with an initial intrusion temperature well in excess of 925 °C. Such an initial intrusion temperature is inconsistent with the available geothermometry results from both the marbles and the stock and probably exceeds the maximum possible liquidus temperature for a granodiorite magma as well. The presence of stable, euhedral hornblende in the stock (Wilson, 1961) at the low pressures indicated for the Alta aureole (<200 MPa) would require a H_2O content in the magma in excess of 5 wt% (Merzbacher and Eggler, 1984; Rutherford and Devine, 1988). This implies that the magma was at, or very near, H_2O saturation when it was intruded. The maximum possible temperature for intrusion of the Alta stock then corresponds to the H_2O-saturated liquidus temperature for a granodiorite magma at low pressures (<150 MPa), which is approximately 960 °C (Rutherford and Devine, 1988). Such a high intrusion temperature directly contradicts the geothermometry evidence from both the stock and the aureole.

If an initially hotter stock cannot account for the observed discrepancy, then an alternative mechanism to elevate the model thermal profile is an increase in the preintrusive wall-rock temperature (T_o). At a minimum, T_o would have to be increased to >375–400 °C to eliminate the discrepancies between model results and the lower limit of uncertainty in the geothermometry data (Fig. 7) throughout the aureole, not just in the outer aureole where the effects of increasing T_o are the greatest.

However, there are geologic, petrologic, and thermal factors that constrain T_o to much less than 375 °C. The preintrusive geothermal gradient of 55 °C/km selected for the model and the resulting T_o = 275 °C at the depth of the sampled section of the contact aureole (−5.2 to −5.5 km) are already significantly elevated values compared with those (30 °C/km and T_o = 165 °C) appropriate for the regional tectonic setting of the Wasatch range and for the estimated depth of emplacement (3–6 km) of the Alta stock (Wilson, 1961; Cook, 1992). These elevated values were selected to accommodate the possible thermal effects of previous intrusive activity in the area (Crittenden et al., 1973).

Initial wall-rock temperatures of ≥375–400 °C are also inconsistent with the absence of the regional development of either talc or tremolite in these siliceous dolomites. At the very H_2O-rich pore fluid compositions ($X_{CO_2} \ll 0.03$) characteristic of deep ground waters in sedimentary sequences prior to the onset of metamorphic reactions (for example, Hitchon and Friedman, 1969), thermodynamic calculations show that the first appearance of talc would be below 325 °C. If the actual initial temperatures at Alta were in the vicinity of 375–400 °C required to eliminate most of the discrepancy between model results and the lower limits to geothermometry, then there should be widespread evidence of regional low-grade metamorphism (ubiquitous presence of talc and even tremolite) in the siliceous dolomites stratigraphically equivalent to those in the aureole. No such regional metamorphism is observed in this area of the Wasatch range, nor has it been reported in the literature; on the contrary, the spatial distribution of both tremolite and talc in these protoliths is clearly related to the Alta, Little Cottonwood, and Clayton Peak stocks and therefore is contact metamorphic in origin.

Finally, if the thermal profile recorded in the Alta aureole is ascribed solely to conductive heat transport from the Alta stock, then basic heat flow-balance considerations for conduction require specific relationships among intrusion (T_m), contact (T_c), and initial wall-rock (T_o) temperatures. These basic considerations (Turcotte and Schubert, 1982, p. 168–172) can be summarized by the following generalization:

$$T_c = x(T_m - T_o) + T_o \quad (10)$$

where the specific value of the coefficient x depends on the thermal properties of the intrusion and wall rocks, the amount of latent heat of crystallization assigned to the intrusion, and the initial difference in temperature between magma and wall rock. For many common rock and magma types intruded into the shallow crust, values of x are close to 0.6 (Turcotte and Schubert, 1982, p. 172). The value of the coefficient x increases with an increasing difference between T_m and T_o and with increas-

ing latent heat of crystallization. For the specific situation at Alta, $x > 0.61$ even for the geologically unrealistic situation of $T_o = 0$ °C. For the likely minimum possible T_o at Alta, 100 °C (based on a minimum estimated depth of emplacement = 3 km and an unperturbed geothermal gradient of 30 °C/km), $x = 0.623$. Equation 10 is routinely invoked to make estimates of T_c, on the basis of known or assumed values of T_m and T_o. However, if both T_m and T_c are known from applications of geothermometry, then these same heat balance relationships establish rather firm upper limits to T_o for any model of the thermal evolution of an aureole that invokes strictly conductive heat transport.

The second-order polynomial fit to the geothermometry data in the Alta aureole defines $T_c = 626$ °C (Fig. 3). With $T_c = 626$ °C, $T_m = 825$ °C on the basis of the results of zirconium geothermometry, and $x = 0.61$, Equation 10 yields an upper limit to $T_o = 325$ °C (for the more realistic value of $x = 0.623$, the maximum T_o would be 300 °C). This upper limit to T_o is only somewhat higher than that ($T_o = 275$ °C) used in the previous model calculations (curves A and B: Fig. 7). Use of this upper limit to T_o (325 °C) would yield model temperatures for the outer aureole that are still 60 °C below the measured thermal profile (but close to the lower limits of uncertainty). Such an increase is also inadequate to remove significant discrepancies (up to 75 °C) between model results and measured temperatures throughout much of the rest of the contact aureole. Thus these geologic, petrologic, and thermal considerations suggest that a geologically realistic increase in T_o alone is a very unlikely mechanism by which to resolve the large discrepancy between the conductive model results and geothermometry data.

If the large discrepancy between the thermal profiles predicted by conductive cooling models for the stock and the observed thermal profile defined by geothermometry and phase equilibria cannot be resolved by geologically reasonable increases in intrusion and wall-rock temperatures alone, then these discrepancies must be due to one or more of the following possibilities: (1) increase in the height of the stock, (2) thermal effects of magma convection, (3) hidden intrusions or dipping igneous contact beneath the aureole, (4) advective heat effects.

Increase in the vertical extent of the stock. One possibility is that the top of the stock is significantly higher than the top of the stock in the thermal model. The two-dimensional results indicate that the largest increases in wall-rock temperatures occur in the region below the midpoint of the stock's vertical margin (Fig. 6). If the stock had had a greater vertical extent in the model, then the carbonate stratigraphic section exposed in the contact aureole would have been located lower relative to the midpoint of the stock's vertical margin and would have been placed in a higher temperature regime (Fig. 6). As constructed, the model already has a postulated 0.3 km of additional vertical extent beyond the present erosional exposure. The top of the stock would still have to be raised by $\gg 1$ km to account for the discrepancy of >100 °C in temperature between observed and model thermal profiles. The occurrence of several roof pendants within the stock (Fig. 1) suggests that the present erosional exposure lies near the original upper margin of the stock. However, a significantly greater vertical extent than that already included in the model cannot be completely ruled out.

Thermal effects of magma convection. Magma convection can affect maximum temperatures in a contact aureole (Jaeger, 1964). In attempting to simulate vigorous magma convection, Bowers et al. (1990) found that the effects of magma convection on maximum temperature-distance profiles normal to the igneous contacts of planar or regular geometry (analogous to the south contact of the Alta stock) were minor, except very near the igneous contact. However, they did find that the effects are more significant locally near geometric irregularities in an igneous contact (reentrants and apophyses). Some magma convection may have occurred in the Alta stock, on the basis of local occurrences of flow banding. We cannot evaluate quantitatively the effect of magma convection because of the lack of information with which to define actual convection parameters appropriate for the Alta stock. On the basis of the numerical experiments of Bowers et al. (1990), it is likely that the effects of magma convection on the temperature-distance profiles for the south Alta aureole would be relatively small, given the regular, vertical geometry of the south contact (Figs. 1 and 2).

Hidden intrusions. The occurrence of hidden intrusive masses or dipping igneous contacts beneath wall rocks can exert significant effects on temperature. There is no geological evidence in either outcrop or mine workings for intrusions underlying or near the south part of the Alta aureole in the areas sampled for geothermometry. Outcrop patterns indicate that for the level of the aureole exposed, the contact of the Alta stock is nearly vertical and regular. In addition, isograds parallel this igneous contact (Moore and Kerrick, 1976; Fig. 1 of this paper) and show no evidence of perturbation by hidden intrusions. As there is no geological evidence for hidden intrusions, this possibility is speculation and is not a testable hypothesis.

Advective heat effects. Advective heat transport may also increase temperatures in the aureole (Cathles, 1977; Norton and Knight, 1977; Parmentier and Schedl, 1981; Furlong et al., 1991). The possibility that advective heat transfer contributed significantly to the thermal evolution of this section of the aureole is particularly attractive because of independent field, petrologic, and stable isotopic evidence for the occurrence of infiltration-driven metamorphism.

Geologic, petrologic, and isotopic evidence for fluid flow

Consider the formation of periclase by the reaction

$$\text{Do} = \text{Per} + \text{Cc} + \text{CO}_2. \quad (6)$$

In a closed system, a prograde reaction can only advance

as long as temperature rises, and, correspondingly, a prograde reaction can only buffer the pore fluid composition to higher X_{CO_2} values as long as temperature continues to rise. Once a rock reaches a maximum temperature, no additional reaction can occur. At the pressure conditions estimated for the Alta aureole (P_f = 75–100 MPa), very little periclase can be produced under closed system conditions unless temperatures exceed the steep-sloped portion of the T-X_{CO_2} equilibrium surface for Reaction 6, or above approximately 700 °C. Thus the formation of a significant quantity of periclase without infiltration by a H_2O-rich fluid requires temperatures well in excess of 700 °C. Such high temperatures near the igneous contact are precluded by the conductive cooling models of the stock, on the basis of the estimated intrusion temperature of the magma (approximately 825 °C) and the results of calcite + dolomite geothermometry.

Yet many of the marbles contain abundant periclase and are nearly devoid of dolomite, indicating that Reaction 6 has gone nearly to completion in these samples. This discrepancy between observed reaction progress and the limited abundance of periclase predicted for closed-system conditions requires infiltration of a significant volume of H_2O-rich fluid (Cook, 1992) to permit the formation of periclase at more reasonable temperatures ($\leq$600 °C) by displacing and diluting CO_2 generated by the reaction.

The spatial distribution of periclase within the periclase zone indicates that this infiltration was largely lateral to the intrusive contact. Within the periclase zone the original bedding in the marbles is almost horizontal (0–10°W dip) when corrected for postintrusion rotation on the Wasatch fault and is nearly perpendicular to the intrusive contact. Throughout the zone, periclase-bearing beds alternate with periclase-absent beds. This pattern is inconsistent with vertical flow through this zone, requiring that fluid flow was bedding-controlled and largely lateral to the vertical intrusive contact. A lateral flow pattern is further supported by the metasomatic introduction of bedding-concordant ludwigite and thin garnet-pyroxene skarn layers within individual periclase-bearing beds.

Lateral infiltration by a significant amount of ^{18}O-depleted fluid is also required by stable isotope data. Much of the periclase zone is significantly depleted in ^{18}O (up to 16‰: Cook, 1992). These depletions are far too large to result from isochemical decarbonation alone (Valley, 1986) and require the infiltration of a significant quantity of ^{18}O-depleted fluid. Within the ^{18}O-depleted periclase zone there are also significant bed to bed variations in $\delta^{18}O$ values (Cook, 1992). As with the distribution of periclase, this pattern of ^{18}O depletion is inconsistent with vertical flow in the periclase zone and requires that fluid flow was bedding-controlled and largely lateral to a nearly vertical igneous contact. The most ^{18}O-depleted calcites have $\delta^{18}O$ values (8–10‰) equivalent to those in exchange equilibrium with the Alta stock (8–9‰), implying that the fluids equilibrated isotopically with the adjacent Alta stock prior to infiltrating the periclase zone.

Application of one-dimensional isotope transport models indicate that the observed pattern of ^{18}O depletion in the south aureole (Cook, 1992) is inconsistent with fluid flow toward the igneous contact (i.e., in the direction of increasing temperature) (Bowman et al., 1994). Rather, transport modeling demonstrates that the observed isotopic patterns are consistent with the flow of significant amounts of ^{18}O-depleted fluid laterally away from the igneous contact (i.e., in the direction of decreasing temperature) (Bowman et al., 1994), a conclusion consistent with the geothermometry data and thermal modeling results presented here. Application of one-dimensional flow models is justified by the field, petrologic, and isotopic evidence indicating one-dimensional (i.e., bedding-controlled) flow in the marbles.

Numerical models (two-D, axisymmetric) of advective heat transport require cumulative fluid flux approximating 10^3 to 3×10^3 m^3/m^2 and time scales of approximately 5×10^3 yr to match the observed calcite + dolomite thermometry profile and to reproduce the observed width of the periclase zone (Cook, 1992). One-dimensional models of O isotope transport require a minimum cumulative fluid flux of approximately 8×10^2 m^3/m^2 to reproduce the observed patterns of ^{18}O depletion in the dolomitic marbles of the south aureole (Bowman et al., 1994). This flux estimate is a minimum one because in an axisymmetric aureole such as the Alta aureole flowlines are radial, not parallel. The general consistency of these flux estimates lends credence to the possibility that fluid flow has systematically affected the thermal regime of the southern part of Alta aureole at the level of current exposure.

Summary

The main points of this study can be summarized as follows:

1. Calcite + dolomite geothermometry applied to siliceous dolomites in the contact aureole of the Alta stock constrains the temperature of metamorphism to the range 410–575 °C. These temperatures are compatible with temperature limits from phase equilibria for the observed mineral assemblages.

2. The minimum temperature recorded by calcite + dolomite geothermometry for the formation of periclase (575 °C) requires a minimum fluid pressure of approximately 75 MPa during the metamorphic event. However, if 575 °C is close to the actual peak temperature achieved at the periclase isograd, the fluid pressures during the event must have been considerably less than the estimated lithostatic pressure of 150 MPa.

3. The temperature-distance profile recorded by calcite + dolomite pairs for the exposed level of the south aureole is significantly hotter at all distances than maximum temperature profiles computed from geologically reasonable, conductive cooling models of the Alta stock that utilize initial magma and wall-rock temperatures consistent with available petrologic and geologic evidence.

4. This significant and systematic discrepancy throughout the aureole suggests one or more possibilities: (1) this section of the aureole formed at a much greater depth relative to the top of the intrusion than estimated; (2) magma convection significantly affected the thermal profile; or (3) the observed thermal profile was affected by advective heat transfer.

5. The possibility of advective heat transport is particularly attractive, with the field observations, petrological constraints on the formation of periclase, spatial patterns of $\delta^{18}O$ values (Cook, 1992), and isotope transport modeling results (Bowman et al., 1994), which independently indicate extensive, bedding-controlled fluid infiltration lateral to the intrusive contact during prograde metamorphism. The similarity of flux estimates from independent heat transfer and mass (O isotope) transport models (Cook, 1992; Bowman et al., 1994) required to reproduce the observed thermal and isotopic characteristics of the marbles lends credence to the possibility that fluid flow has systematically affected the thermal regime of the southern part of Alta aureole at the level of current exposure.

Acknowledgments

We thank Lukas Baumgartner and an anonymous reviewer for their constructive reviews. This study represents a portion of the senior author's Ph.D. dissertation at the University of Utah. Financial support for this study was provided by NSF grants EAR-8904948 and EAR-9205085 to J.R.B. Additional support was provided by the University of Utah Mining and Mineral Resources Research Institute in the form of a research fellowship to the senior author.

References cited

Anovitz, L.M., and Essene, E.J. (1987) Phase equilibria in the system $CaCO_3$-$MgCO_3$-$FeCO_3$. Journal of Petrology, 28, 389–414.

Baker, A.A., Calkins, F.C., Crittenden, M.D., and Bromfield, C.S. (1966) Geologic map of the Brighton quadrangle, Utah. U.S. Geological Survey Map GQ-535.

Bebout, G.E., and Carlson, W.D. (1986) Fluid evolution and transport during metamorphism: Evidence from the Llano Uplift, Texas. Contributions to Mineralogy and Petrology, 92, 518–529.

Bowers, J.R., Kerrick, D.M., and Furlong, K.P. (1990) Conduction model for the thermal evolution of the Cupsupic aureole, Maine. American Journal of Science, 290, 644–665.

Bowers, T.S., and Helgeson, H.C. (1983) Calculation of the thermodynamic and geochemical consequences of nonideal mixing in the system H_2O-CO_2-NaCl on phase relations in geologic systems: Equation of state for H_2O-CO_2-NaCl fluids at high pressures and temperatures. Geochimica et Cosmochimica Acta, 47, 1247–1275.

Bowman, J.R., and Essene, E.J. (1982) P-T-$X(CO_2)$ conditions of contact metamorphism in the Black Butte aureole, Elkhorn, Montana. American Journal of Science, 282, 311–340.

Bowman, J.R., Willett, S.D., and Cook, S.J. (1994) Oxygen isotopic transport and exchange during fluid flow: One-dimensional models and applications. American Journal of Science, 294, 1–55.

Calkins, F.C., and Butler, B.S. (1943) Geology and ore deposits of the Cottonwood-American Fork district, Utah. U.S. Geological Survey Professional Paper, 201, 154 p.

Carslaw, H.S., and Jaeger, J.C. (1959) Conduction of heat in solids, p. 510. Clarendon, Oxford, U.K.

Cathles, L.M. (1977) An analysis of the cooling of intrusives by groundwater convection which includes boiling. Economic Geology, 72, 804–826.

Cook, S.J. (1992) Contact metamorphism surrounding the Alta stock, Little Cottonwood Canyon, Utah. Ph.D. thesis, University of Utah, Salt Lake City, Utah.

Crittenden, M.D. (1965) Geology of the Dromedary Peak quadrangle, Utah. U.S. Geological Survey Map GQ-378.

Crittenden, M.D., Stuckless, J.S., Jr., Kistler, R.W., and Stern, T.W. (1973) Radiometric dating of intrusive rocks in the Cottonwood area, Utah. U.S. Geological Survey Journal of Research, 1, 173–178.

Duffy, C.J., and Greenwood, H.J. (1979) Phase equilibria in the system MgO-MgF_2-SiO_2-H_2O. American Mineralogist, 64, 1156–1174.

Essene, E.J. (1989) The current status of thermobarometry in metamorphic rocks. In Geological Society of America Special Paper, 43, 1–44.

Ferry, J.M. (1980) A case study of the amount and distribution of heat and fluid during metamorphism. Contributions to Mineralogy and Petrology, 71, 373–385.

——— (1983) On the control of temperature, fluid composition, and reaction progress during metamorphism. American Journal of Science, 283-A, 210–232.

——— (1989) Contact metamorphism of roof pendants at Hope Valley, Alpine County, California, USA: A record of the hydrothermal system of the Sierra Nevada batholith. Contributions to Mineralogy and Petrology, 101, 402–417.

Furlong, K.P., Hanson, R.B., and Bowers, J.R. (1991) Modeling thermal regimes: In Mineralogical Society of America Reviews in Mineralogy, 26, 437–506.

Giberti, G., Moreno, S., and Sartoris, G. (1984) Evaluation of approximations in modeling the cooling of magmatic bodies. Journal of Volcanology and Geothermal Research, 20, 297–310.

Helgeson, H.C., Delaney, J.M., Nesbitt, H.W., and Bird, D.K. (1978) Summary and critique of the thermodynamic properties of rock-forming minerals. American Journal of Science, 278A, 1–228.

Hintze, L.F. (1973) Geologic history of Utah. Brigham Young University Geology Studies, 20, 1–181.

Hitchon, B., and Friedman, I. (1969) Geochemistry and origin of formation waters in the western Canada sedimentary basin. I. Stable isotopes of hydrogen and oxygen. Geochimica et Cosmochimica Acta, 33, 1321–1349.

Hover-Granath, V.C., Papike, J.J., and Labotka, T.C. (1983) The Notch Peak contact metamorphic aureole, Utah: Petrology of the Big Horse Limestone member of the Orr Formation. Geological Society of America Bulletin, 94, 889–906.

Huyakorn, P.S., and Pinder, G.F. (1983) Computational methods in subsurface flow, p. 39–42. Academic, Orlando, Florida.

Jaeger, J.C. (1964) Thermal effects of intrusions. Reviews in Geophysics and Space Physics, 2, 443–466.

John, D.A. (1991) Evolution of hydrothermal fluids in the Alta stock, Central Wasatch Mountains, Utah. U.S. Geological Survey Bulletin, 1977, 51 p.

Keenan, J.H., Keyes, F.G., Hill, P.G., and Moore, J.G. (1978) Steam tables. Wiley, New York.

Kemp, W.M., III (1985) A stable isotope and fluid inclusion study of the contact Al(Fe)-Ca-Mg-Si skarns in the Alta Stock aureole, Alta, Utah, 65 p. M.S. thesis, University of Utah, Salt Lake City, Utah.

Kestin, J. (1978) Thermal conductivity of water and steam. Mechanical Engineering, 100, 1255–1258.

Merzbacher, C., and Eggler, D.H. (1984) A magmatic geohydrometer, applications to Mount St. Helens and other dacitic magmas. Geology, 12, 587–590.

Meyer, C.A., McClintoch, R.B., Silvestri, G.J., and Spencer, R.C. (1967) ASME steam tables: Thermodynamic and transport properties of steam. American Society of Mechanical Engineers, New York.

Moore, J.N., and Kerrick, D.M. (1976) Equilibria in siliceous dolomites of the Alta aureole, Utah. American Journal of Science, 276, 502–524.

Nabelek, P.I., Labotka, T.C., O'Neil, J.R., and Papike, J.J. (1984) Contrasting fluid/rock interaction between Notch Peak granitic intrusion and argillites and limestones in western Utah: Evidence from stable isotopes and phase assemblages. Contributions to Mineralogy and Petrology, 86, 25–34.

Norton, D., and Knight, J. (1977) Transport phenomena in hydrothermal systems: Cooling plutons. American Journal of Science, 277, 937–981.

Parmentier, E.M., and Schedl, A. (1981) Thermal aureoles of igneous intrusions: Some possible indications of hydrothermal convective cooling. Journal of Geology, 89, 1–22.

Pouchou, J-L., and Pichoir, F. (1991) Quantitative analysis of homogeneous or stratified microvolumes applying the model "PAP". In K.F.J. Heinrich and D.E. Newberry, Eds., Electron probe quantitation, p. 31–75. Plenum, New York.

Rice, J.M. (1977) Contact metamorphism of impure dolomitic limestone in the Boulder aureole, Montana. Contributions to Mineralogy and Petrology, 59, 237–259.

Rice, J.M., and Ferry, J.M. (1982) Buffering, infiltration and control of intensive variables during metamorphism. In Mineralogical Society of America Reviews in Mineralogy, 10, 263–326.

Robie, R.A., Hemingway, B.S., and Fisher, J.R. (1978) Thermodynamic properties of minerals and related substances at 298.15K and 1 bar (10^5 pascals) pressure and at higher temperatures. U.S. Geological Survey Bulletin, 1452, 456 p.

Rutherford, M.J., and Devine, J.D. (1988) The May 18, 1980 eruption of Mount St. Helens. III. Stability and chemistry of amphibole in the magma chamber. Journal of Geophysical Research, 93, 11949–11959.

Smith, R.K. (1972) The mineralogy and petrology of the contact metamorphic aureole around the Alta stock, Utah. Ph.D. thesis, University of Iowa, Iowa City, Iowa.

Straus, J.M., and Schubert, G. (1977) Thermal convection of water in a porous medium: Effects of temperature- and pressure-dependent thermodynamic and transport properties. Journal of Geophysical Research, 82, 325–333.

Turcotte, D.L., and Schubert, G. (1982) Geodynamics: Applications of continuum physics to geological problems, p. 168–172. Wiley, New York.

Valley, J.W. (1986) Stable isotope geochemistry of metamorphic rocks. In Mineralogical Society of America Reviews in Mineralogy, 16, 445–489.

Valley, J.W., and Essene, E.J. (1980) Calc-silicate reactions in Adirondack marbles: The role of fluids and solid solutions. Geological Society of America Bulletin, 91, 114–117, 720–815.

Watson, E.B., and Harrison, T.M. (1983) Zircon saturation revisited: Temperature and composition effects in a variety of crustal magma types. Earth and Planetary Science Letters, 64, 295–304.

Wilson, J.W. (1961) Geology of the Alta stock. Ph.D. thesis, California Institute of Technology, Pasadena, California.

Woodside, W.H., and Messmer, J.H. (1961) Thermal conductivities of porous media. II. Consolidated rocks. Journal of Applied Physics, 32, 1699–1706.

Manuscript received March 29, 1993
Manuscript accepted January 19, 1994